Published in final edited form as:
Eur J Neurosci. 2012 September ; 36(6): 2773–2781. doi:10.1111/j.1460-9568.2012.08204.x.

Altered spatial learning, cortical plasticity and hippocampal anatomy in a neurodevelopmental model of schizophrenia-related endophenotypes

P. Leon Brown[1,2], **Paul D. Shepard**[1], **Greg I. Elmer**[1], **Sara Stockman**[1], **Rebecca McFarland**[1], **Cheryl L. Mayo**[1], **Jean Lud Cadet**[3], **Irina N. Krasnova**[3], **Martin Greenwald**[1], **Carrie Schoonover**[1], and **Michael W. Vogel**[1]

[1]Maryland Psychiatric Research Center, Department of Psychiatry, Baltimore, MD, USA

[2]Program in Neuroscience, University of Maryland School of Medicine, Baltimore, MD, USA

[3]Molecular Neuropsychiatry Research Branch, Intramural Research Program, National Institute on Drug Abuse, NIH, DHHS, Baltimore, MD, USA

Abstract

Adult rats exposed to the DNA-methylating agent methylazoxymethanol on embryonic day 17 show a pattern of neurobiological deficits that model some of the neuropathological and behavioral changes observed in schizophrenia. Although it is generally assumed that these changes reflect targeted disruption of embryonic neurogenesis, it is unknown whether these effects generalize to other antimitotic agents administered at different stages of development. In the present study, neurochemical, behavioral and electrophysiological techniques were used to determine whether exposure to the antimitotic agent Ara-C later in development recapitulates some of the changes observed in methylazoxymethanol (MAM)-treated animals and in patients with schizophrenia. Male rats exposed to Ara-C (30 mg/kg/day) at embryonic days 19.5 and 20.5 show reduced cell numbers and heterotopias in hippocampal CA1 and CA2/3 regions, respectively, as well as cell loss in the superficial layers of the pre- and infralimbic cortex. Birth date labeling with bromodeoxyuridine reveals that the cytoarchitectural changes in CA2/3 are a consequence rather that a direct result of disrupted cortical neurogenesis. Ara-C-treated rats possess elevated levels of cortical dopamine and DOPAC (3,4-didyhydroxypheylacetic acid) but no change in norepinephrine or serotonin. Ara-C-treated rats are impaired in their ability to learn the Morris Water Maze task and showed diminished synaptic plasticity in the hippocampocortical pathway. These data indicate that disruption of neurogenesis at embryonic days 19.5 and 20.5 constitutes a useful model for the comparative study of deficits observed in other gestational models and their relationship to cognitive changes observed in schizophrenia.

Keywords

animal model; cytosine arabinoside; long-term potentiation; methylazoxymethanol; rat; spatial learning

Correspondence: Dr M. W. Vogel.

[*]*Present address*: Office of Research Training and Career Development, Division of Neuroscience & Basic Behavioral Science, National Institute of Mental Health, 6001 Executive Blvd, Bethesda, MD 20892-9645, USA.

Introduction

The complex clinical presentation and unknown etiology of schizophrenia present significant challenges to the development of heuristic animal models of this disorder. Models based on pharmacological or genetic manipulations induce behavioral changes indicative of specific features of this illness but are often limited to perturbations in a single neurotransmitter system or specific genetic loci and do not reproduce the spectrum of deficits that characterize the idiopathic form of the disorder (Boksa, 2007; Low & Hardy, 2007).

The reconceptualization of schizophrenia as a neurodevelopmental disorder has led to the creation of a new class of animal models that invoke specific pre- or perinatal insults associated with an increased risk of developing the disorder as an adult (Meyer & Feldon, 2010; Jones *et al*., 2011). Epidemiologically based neurodevelopmental models of schizophrenia include maternal nutritional deficiency, obstetric complication, exposure to stress and immune activation (Meyer & Feldon, 2010). These models place particular emphasis on differentiating behavioral changes that are manifest immediately from those which appear during or following adolescence and thus better correspond to the ontogeny of the illness in humans. Transient inhibition of neurogenesis via maternal exposure to antimitotic agents has also been used successfully to investigate the delayed sequelae associated with focal disruption of brain development (Elmer *et al*., 2004; Lodge & Grace, 2009; Moore, 2010). Although lacking the construct validity of epidemiologically based models, the approach offers the advantage of targeting specific groups of neurons, based on their ontogeny, during a particular stage of their development.

Prenatal administration of the mitotic inhibitor cytosine arabinoside (Ara-C), inhibits DNA synthesis resulting in transient suppression of neurogenesis (Sarraf *et al*., 1993; Gmeiner *et al*., 1998; Courtney & Coffey, 1999). In a previous study, we found that rats exposed to Ara-C *in utero* at embryonic day (E)19.5 and 20.5 showed diminished sensory gating, lower acoustic startle and a subtle disorganization of the pyramidal cell layer in the CA2/3 region of the hippocampus as adults (Elmer *et al*., 2004). This point in development, which coincides with the end of hippocampal and neocortex neurogenesis (Bayer *et al*., 1993), corresponds to the beginning of the second trimester in human pregnancy, a time of elevated epidemiological vulnerability for the development of schizophrenia (Fatemi & Folsom, 2009).

In the present experiments, we sought to extend our initial assessment of the changes in Ara-C-treated animals to provide insight into the nature of the anatomical disruption and its possible effect on hippocampal-dependent cognitive tasks. To accomplish this, bromodeoxyuridine (BrdU) labeling techniques were used to determine the effects of E19.5 and 20.5 Ara-C injections on hippocampal and cortical neurogenesis. Spatial learning and memory deficits induced by Ara-C were assessed using the Morris water maze (MWM), and the functional integrity of the connections between the prefrontal cortex and hippocampus were probed by comparing changes in synaptic plasticity within the hippocampocortical pathway. Our results show that Ara-C applied during this crucial neurodevelopmental window alters hippocampal-dependent behavior and the functional connectivity of a circuit that has been implicated in the disorder.

Methods

Subjects

Sprague-Dawley rat dams (Charles River) were delivered to the animal facilities at the Maryland Psychiatric Research Center on the second day of pregnancy and maintained on a

12:12-h light–dark cycle with food and water provided *ad libitum*. Dams were injected with either Ara-C (30 mg/kg, i.p. in PBS) or PBS alone on the morning of E19.5 and E20.5. Pups were weaned at postnatal day (PND) 21 and male offspring were group housed (2–3 per cage by litter) with *ad lib* access to food and water. All tests were conducted in adult (> PND 56) male offspring. All animal protocols were approved by the University of Maryland, Baltimore Institutional Animal Care and Use Committee.

BrdU labeling

A group of male rats treated with Ara-C (*n*=8) or saline (*n*=8) but not subjected to behavioral or electrophysiological testing were used in these studies. Rat dams were administered BrdU (50 mg/kg i.p. in 0.001 M NaOH) concurrently with Ara-C (30 mg/kg or saline) at E19.5 and E20.5. The BrdU-treated rats were killed as adults by cardiac perfusion with an acetic acid/alcohol fixative (1:3). Fixed brains were dehydrated, embedded in paraffin, sectioned serially at 25 μm and mounted on glass slides in a sequential series. Sections on systematically randomly selected slides were dewaxed, hydrated and processed for BrdU histochemistry using a variation of previously established immunohistochemical protocols (Vogel *et al*., 2000). In brief, sections were incubated with (a) 0.3% H_2O_2 in methanol for 10 min, and rinsed twice in dH_2O, (b) citric acid unmasking agent (Vector Laboratories) at 90°C for 20 min, (c) 1 M HCl at 37 °C for 30 min, and (d) 0.1 M Borax for 10 min. The sections were then washed in dH_2O, followed by two rinses in 50 mM Tris-buffered saline for 5 min and then two rinses of 0.3% Tween in Tris-buffered saline (5 min each). The sections were blocked in 0.3% Tween in Tris-buffered saline and 3% normal goat serum for 30 min and incubated overnight in mouse anti-BrdU monoclonal antibody (dilution 1:25 in PBS; Becton-Dickinson). Sections were rinsed three times in PBS and a peroxidase-conjugated secondary antibody was reacted with the sections for 2 h in a humidified chamber at room temperature (Vectastain kit). Slides were rinsed in Tris-buffered saline and the peroxidase revealed with diaminobenzidine (0.05%) and H_2O_2 (0.005%). Slides that were processed for BrdU histochemistry were not counter-stained before mounting permanently, but the neighboring slides were dewaxed and counter-stained with cresyl violet to aid in the identification of brain regions containing BrdU-labeled cells. The number of BrdU-labeled nuclei in the ventral hippocampus and prelimbic–infralimbic (PrL-IL) cortex was surveyed using stereological techniques. These regions corresponded to the areas used to assess cortical long-term potentiation. Briefly, Stereologer (SPA Inc., Alexandria, VA, USA) was used to systematically sample each section randomly with a counting grid using the following parameters: the dissector frame area was 200 μm^2 × 12 μm deep with a guard height of 1 μm and dissector frames were spaced 100 μm apart. A standard volume for each brain region was profiled in each experimental group (saline, AraC). The atlas of Paxinos & Watson (2007) was used as a reference to outline the PrL-IL cortex (interaurally 12.72–11.76 mm, from a dorsal–ventral position of 2.8–5.0 mm and from the medial line to the forceps minor of the corpus callosum in the medial–lateral plane) and the ventral hippocampus [interaurally 3.12–2.56 mm, from a dorsal–ventral position of 4.0–7.0 mm and from the medial outline of the granular layer of the dentate gyrus (~4.8 mm) to the lateral outline of the oriens layer of the hippocampus (6.2 mm)]. Counting was accomplished using an Olympus BH-2 microscope with Nomarski optics and a 100x objective to project an image of the section on a computer. The number of BrdU-labeled nuclei was averaged across an equal number of brain slices taken within each region of interest for each animal. The estimated number of BrdU-labeled nuclei per animal per treatment and brain region were log-transformed and analysed via one-way ANOVA.

The number of pyramidal neurons in hippocampal regions CA1 and CA2/3 on the opposite side of the brain were also estimated in cresyl violet-stained sections using stereological techniques as described previously (West *et al*., 1991). Only large neurons with a pyramidal

shape and nuclei larger than 8 μm were counted. The following parameters were used to estimate neuronal number: the dissector frame area was 737 μm^2 × 12 μm deep with a guard height of 3 μm and dissector frames were spaced 200 μm apart. The section-sampling fraction was 0.0833 (15 sections analysed per brain with a sampling interval of 12) and the area-sampling fraction was 0.018. The brains were sectioned at 25 μm in paraplast. After processing, the average section thickness was 23.2 ± 0.18 μm, so the thickness sampling fraction was 0.514 ± 0.004. These counting parameters provided for counts of over 100 pyramidal neurons per hippocampal region (CA1 average = 126 ± 5.16 neurons, C.E. = 0.09 ± 0.002; CA2/3 average = 183 ± 10.6 neurons, C.E. = 0.076 ± 0.002). Counts were conducted using an Olympus BH-2 microscope with Nomarski optics and a 100x objective to project an image of the section on a computer (MacIntosh G3). Hippocampal volumes for the CA1 and CA2/3 regions were estimated using the Cavalieri estimator of volume.

Neurochemistry

Frontal cortices dissected from PND 56 rats were homogenized in 0.01 M $HClO_4$ and centrifuged at 18,000***g*** for 15 min. Norepinephrine, dopamine (DA), 3,4-didyhydroxypheylacetic acid (DOPAC), homovanillic acid, serotonin and 5-hydroxyindoleacetic acid were measured by high-performance liquid chromatography with electrochemical detection as previously described (Krasnova *et al*., 2010). Monoamine concentrations were expressed as pg/mg of tissue weight. Comparisons between control (saline) and Ara-C-treated groups were made using a Student's t-test.

Behavioral testing

A different group of subjects were evaluated for spatial navigation capacity using a MWM procedure (Morris, 1984). Testing was conducted in a circular fiberglass pool (1.8 m diameter, 0.9 m high) filled to a depth of 0.6 m with water (21 ± 1.0 °C) rendered opaque with a non-toxic white paint. Unless otherwise indicated, a translucent acrylic platform (13.5 × 13.5 cm) was positioned inside the pool, 2 cm below water level in the center of the north-west quadrant. The room contained numerous visual cues, in the form of colored shapes, located outside of the maze on the room walls and room partition. A ceiling-mounted video camera connected to a software package (Ethovision) was used to track and record the path taken by the rat. A black triangle was added to the top of each rat's head with permanent hair color prior to habituation and testing to increase reliability of the tracking measurement.

Rats were briefly exposed (2 min) to the pool without the platform on the day prior to the start of behavioral testing in order to habituate the subject to the procedures. Behavioral testing occurred over the next 8 days and consisted of three distinct and consecutive phases.

Acquisition (Days 1–4)—During the acquisition phase, each rat was tested in four trials per day that were randomly initiated at the N, E, S or W coordinate. Start location was run in a counterbalanced order across trials and animals. Each animal was given up to 120 s to locate the hidden platform and was required to stay on it for 15 s. If an animal did not find the platform, it was gently guided to the platform location and made to remain there for 15 s. The inter-trial interval was 120 s. The location of the platform remained the same throughout training.

Probe trial (Day 5)—To further assess spatial navigation strategy, the platform was removed and rats were given 60 s to swim freely during four consecutive trials starting at the N, E, S or W coordinate randomized across subjects.

Visible platform (Day 8)—To assess potential deficits in sensory, motor or motivational processes, rats were evaluated on the 8th day for their ability to swim to a visible platform

located 1.5 cm above the surface of the water. Four consecutive trials were run, starting at the N, E, S or W coordinate, randomized across subjects. Upon reaching the platform, latency was recorded and rats were permitted to remain on the platform for an additional 15 s.

The dependent variables collected from the path plots in each trial were time to locate platform (acquisition trials), percentage time in each quadrant, time spent in close proximity (within 15 cm) to the target location and the number of times the subject crossed the platform location. The latter three variables were collected only during the probe trial. The data were analysed using a two-way repeated-measures ANOVA (Ara-C treatment × training Day as a repeated measure). The probe trial data were analysed using a one-way ANOVA (Ara-C treatment). The visible platform data were analysed using a two-way repeated-measures ANOVA with treatment (Ara-C treatment) as a between-subjects variable and test day as a within-subjects repeated measure.

Cortical long-term potentiation

At least 1 week following completion of the MWM testing, saline and Ara-C-treated rats were tested to determine whether high-frequency stimulation of the ventral hippocampus would result in long-term potentiation (LTP) of field potentials recorded in the PrL-IL cortex (Laroche *et al*., 1990; Jay *et al*., 1995, 2004). The experimenter remained blinded to the treatment condition of each animal until all rats had been tested. Animals were anesthetized with chloral hydrate (400 mg/kg, i.p.), positioned in a stereotaxic apparatus equipped with a feedback-controlled heating pad that was used to maintain body temperature at 36 °C. Small burr holes were drilled in the skull above the right medial prefrontal cortex (mPFC; 3.2 mm anterior to Bregma; 0.8 mm lateral to the midline) and ventral hippocampus (6.5 mm posterior to Bregma; 5.5 mm lateral to the midline). A tungsten microelectrode (FHC, Bowdoin, ME, USA; < 1 MΩ impedance *in vitro*) was lowered into the PrL-IL cortex (–2.4 to –3.7 mm ventral from the cortical surface), while a concentric bipolar stimulating electrode (Rhodes Medical Instruments; 250 μm diameter) was positioned within the ventral hippocampus (–3.5 to –6.5mm ventral from the cortical surface). Extracellular field potentials were amplified, filtered (0.1–1000 Hz) and digitized at 10 kHz for analysis offline. Field potentials in the PrL-IL cortex with an onset latency between 18 and 22 ms were evoked using brief (100 μs), rectangular current pulses applied to the hippocampal stimulating electrode using a constant current stimulator. Stimulus pulses were applied at a rate of 0.033 Hz and the amplitude of the evoked potential was optimized by varying the depth of the stimulating and recording electrodes and intensity of the current pulse (0.2–0.8 mA). Once maximized, the stimulus amplitude was reduced to elicit field potential responses that did not exceed 60–70% of the peak amplitude. Once stabilized, a 30-min period of control responses to individual test pulses was recorded. To induce cortical LTP, two sets of tetanizing stimuli consisting of ten 200-ms trains of rectangular current pulses (100 μs at 250 Hz) with an inter-train interval of 10 s was applied to the ventral hippocampus 10 min apart from each other. Test pulses were resumed and evoked potentials were recorded for an additional 60 min following tetanic stimulation. Data were averaged across 5-min blocks and are presented as a percentage change (± SEM) from a grand mean obtained by averaging response amplitudes across the entire 30-min control period.

At the conclusion of the recording experiments, a continuous DC current was passed through the recording (12 μA, 30 s) and stimulating (0.5 mA, 10 s) electrodes. Rats were deeply anesthetized with pentobarbital sodium (100 mg/kg), transcardially perfused (1.6% potassium ferracyanide in 10% formalin) and the brain removed and sectioned (40 μm) for histological confirmation of the electrode placements.

Results

Neuroanatomy

Exposure of pregnant dams to consecutive daily injections of Ara-C on E19.5 and E20.5 resulted in qualitative and quantitative changes in the cytoarchitectural features of the cortex and hippocampus of male offspring. As illustrated in Fig. 1A and B, the CA2/3 region of the dorsal hippocampus showed a pronounced disruption in the lamination of the pyramidal cell layer (Fig. 1B, arrow). Pyramidal cells were often diffusely distributed within the molecular layer leaving gaps in the pyramidal layer, which also showed evidence of neuronal disorientation. Based on counts of hippocampal pyramidal neurons in adult control rats (Fig. 1C, $n = 6$) and rats treated with Ara-C at E19.5–E20.5 (Fig. 1D, $n = 7$), the mean number of CA1 hippocampal pyramidal neurons was reduced by 21% compared with offspring from saline-treated rats (ANOVA $F_{1,11} = 7.5$, $P < 0.02$; Fig. 1E) and there was a trend toward a reduction in the volume of CA1 (ANOVA $F_{1,11} = 4.0$, P = 0.07; Fig. 1F). With respect to the CA2/3 region of the hippocampus, the number of CA2/3 pyramidal neurons in Ara-C-treated rats was reduced by 16% compared with controls, but only the change in neuronal numbers approached statistical significance (ANOVA $F_{1,11} = 3.6$, $P = 0.08$). This result was surprising given the evident disruption in the pyramidal cell layer in the dorsal portion of CA2/3. However, the disruption in the CA2/3 pyramidal layer was always spatially restricted to the dorsal hippocampus. Thus, the contribution made by the ventral hippocampus to overall CA2/3 pyramidal neuron numbers appears to have diminished the impact of the dysplasia in the dorsal CA2/3 region.

To further evaluate the effects of Ara-C injection on hippocampal and cortical development, we analysed the distribution of BrdU-labeled cells in adult brains. Control (saline-treated) rats showed a wide distribution of BrdU nuclear profile labeling throughout the central nervous system, including selected regions of the hippocampus and superficial layers of the PrL-IL cortex (Fig. 2). In general, the density of BrdU-labeled nuclear profiles and intensity of labeling in the Ara-C-treated rats was reduced compared with control brains, although the pattern of labeling was roughly similar. In the dorsal hippocampus, BrdU-labeled profiles are visible in the CA4 (hilus) and CA1 regions in the control hippocampus, but not in the Ara-C-treated hippocampus (arrowheads; Fig. 2A and B, respectively). One of the regions that did not contain significant numbers of BrdU-labeled nuclei in the control or Ara-C-treated rats was the CA2/3 region of the dorsal hippocampus (Fig. 2A and B, arrows). This indicates that CA2/3 pyramidal neurons were not generated at E19.5/20.5, and the dispersion of CA2/3 pyramidal neurons in Ara-C-treated rats (Fig. 1B) occurs secondary to the effects of Ara-C on disrupting neurogenesis. BrdU-labeled nuclear profiles were also observed in the ventral portion of the hippocampus in both control and Ara-C-treated rats. In this region BrdU labeling was reduced in the Ara-C-treated rats compared with controls ($F_{1,5} = 6.90$, $P = 0.0467$; Fig. 2G).

Prominent BrdU staining was also observed in superficial layers of the PrL-IL cortex in control rats (Fig. 2C, arrow). In control rats, BrdU labeling of nuclear profiles ranged from dark, completely filled nuclei to light staining around the perimeter of the nucleus (Fig. 2E, black and white arrowheads, respectively). By contrast, very few BrdU-labeled nuclear profiles were observed in the equivalent cortical layers in Ara-C-treated rats (Fig. 2D) and these are only lightly labeled (Fig. 2F, white arrowheads). The more lightly labeled nuclear profiles are likely to represent progenitor cells that survived the Ara-C treatment and divided again before differentiating as neurons. BrdU-labeled nuclear profiles were also observed in the PrL-IL cortex where the extent of the labeling was significantly less in Ara-C-treated rats than in controls (Fig 2H; $F_{1,5} = 87.8$, $P = 0.0002$).

Overall, the pattern of BrdU-labeled nuclear profiles in control and Ara-C-treated rats suggests that Ara-C injection on E19.5–E20.5 reduced the number of BrdU-labeled neurons in the hillus and CA1 region of the hippocampus as well as in the PrL-IL cortex of adult offspring. The results also demonstrate that neuronal organization can be disrupted by Ara-C in regions where neurons were not being generated at E19.5/20.5 (e.g. the CA2/3 region).

Neurochemistry

Prenatal exposure to Ara-C resulted in a significant increase in DA (t_{18}= –3.3, $P < 0.005$ and DOPAC (t_{18}= –2.1, $P < 0.05$) levels in the frontal cortex of adult rats relative to age-matched, vehicle-treated controls (Fig. 3). Differences in cortical homovanillic acid levels did not reach statistical significance (AraC vs. Saline: 40 ± 5.3 vs. 28 ± 3.0 pg/mg tissue). Cortical norepinephrine (AraC vs. Saline: 249 ± 9.1 vs. 222 ± 10.1 pg/mg tissue), serotonin (AraC vs. Saline: 387 ± 15.6 vs. 390 ± 17.5 pg/mg tissue) and 5-hydroxyindoleacetic (AraC vs. Saline: 202 ± 6.9 vs. 182 ± 7.0 pg/mg tissue) levels were not altered by Ara-C treatment.

MWM performance

Both control and Ara-C-treated rats were able to successfully learn the navigation task as evidenced by a time-dependent decrease in latency to locate the submerged platform during the four days of task acquisition ($F_{3,36}$ = 40.7, $P < 0.001$; Fig. 4). However, Ara-C-treated rats took longer to learn the task than their saline-treated counterparts as reflected by a significant treatment group ($F_{1,12}$ = 11.1, $P < 0.01$) and treatment by time interaction ($F_{3,36}$ = 5.4, $P < 0.01$). Importantly, both groups had similar latencies to find the platform on the first day of acquisition, suggesting that Ara-C treatment did not result in sensory, perceptual, motoric or motivational deficits. Rather, the differences between groups were limited to days 2, 3 and 4 [$P < 0.05$, Fisher's least significance difference (LSD)] with the saline-treated group learning the task at a faster rate than Ara-C-treated subjects.

The results of the probe test further support the conclusion that Ara-C treatment significantly impaired spatial navigation. As illustrated in Fig. 5, Ara-C-treated rats spent less time in the target quadrant of the water maze searching for the hidden platform than saline-treated rats; the deficit was location dependent, as evidenced by a significant treatment by start location interaction ($F_{3,10}$ = 1.3, $P < 0.05$, Fig. 5A and C). Further analysis of the number of crosses over the area formerly occupied by the platform (Fig. 5A and B) or the mean distance to the area formerly occupied by the target platform (Fig. 5C and D) revealed that the deficit was particularly pronounced when Ara-C-treated rats began the probe test either in the North (crosses; $P < 0.05$, Fisher's LSD) or the East (crosses and mean distance; $P < 0.05$, Fisher's LSD) quadrants (Fig. 5C). Ara-C- and saline-treated rats did not differ in the latency to reach the platform when the platform was visible, further supporting the conclusion that Ara-C treatment did not result in sensory, perceptual or motoric deficits.

Synaptic plasticity

Synaptic plasticity was assessed in 13 rats by recording LTP in the hippocampal–prefrontal pathway. Histological analysis confirmed that all animals included in the analysis had stimulating electrodes positioned within the CA1 region of the ventral hippocampus and recording sites in the PrL-IL cortex (Fig. 6A). Single-pulse stimulation of the hippocampus elicited a triphasic potential consisting of a small upward deflection followed by a large negative wave and rebound positivity (Fig. 6B). In accordance with previous reports, the median latency to onset of the negative-going peak was ~ 18 ms (Laroche *et al*., 1990; Jay *et al*., 1995).

In saline-treated control rats (n=7), tetanic stimulation produced a robust and long-lasting potentiation of the synaptic response in the PrL-IL cortex, as evidenced by a significant

increase in evoked potential amplitude (two-way repeated-measures ANOVA, $F_{17,187}$ = 10.5, P< 0.001; Fig. 6C). The relative increase in the amplitude of responses recorded in control rats 30–60 min after tetanic stimulation averaged 52.5 ± 11.1%. High-frequency stimulation of the ventral hippocampus also produced LTP in the adult offspring of Ara-C-treated rats although the percentage change in evoked potential amplitude was significantly smaller than in controls (17.4 ± 9.3%; t_{11} = 2.4, P < 0.05). Despite a clear disparity in the degree of potentiation between control and Ara-C-treated rats at 30–60 min following stimulation, the group effect fell short of achieving statistical significance in a two-way, repeated-measures ANOVA ($F_{1,11}$ = 4.7, P = 0.053). There was, however, a significant time by group interaction ($F_{17,187}$ = 2.8, P <0.001) with post hoc analysis indicating significantly less potentiation in the Ara-C-treated rats at all but three of the 12 post-tetanic time points (P<0.05, Holm-Sidak, Fig. 6C).

Discussion

An ongoing challenge of research into the causes of schizophrenia has been the development of heuristic animal models (Moore, 2010). One approach has been to use antimitotic agents to disrupt neurogenesis during various stages of gestation and to compare the resultant changes in adult animals with deficits commonly observed in schizophrenia. A consistent finding emerging from this work has been recognition of the importance of dose and timing of prenatal exposure to antimitotic agents in determining the scope of effects observed in adults. Administration of MAM to pregnant dams prior to E15 profoundly disrupts the development of allocortical and limbic structures (Talamini *et al*., 1998, 1999) resulting in gross morphological changes that are not typically observed in schizophrenia (Jones *et al*., 2011). By contrast, transient disruption of neurogensis on E17, 2 days after cortical neogenesis has reached its peak in the rat, results in a more subtle disruption in cortical and limbic cytoarchitecture accompanied by a spectrum of behavioral and physiological changes consistent with those observed in schizophrenia (Moore *et al*., 2006; Lodge & Grace, 2009; Jones *et al*., 2011). In addition to developmental timing, the pharmacokinetic and pharmacodynamic properties of the agent used to interrupt mitosis are likely to contribute to its scope and pattern of effects in adults. With the exception of one earlier report (Elmer *et al*., 2004), the majority of studies targeting late gestational neurogenesis in the rat have used MAM. While MAM's antimitotic and antiproliferative actions derive from aberrant DNA methylation, it has also been shown to have long-lasting effects on DNA stability and gene expression in post-mitotic neurons (Esclaire *et al*., 1999). Here, we show that prenatal exposure to Ara-C, a pyrimidine antimetabolite which induces apoptosis in dividing cells by inhibiting DNA synthesis in the S-phase of the cycle, at E19.5–20.5 induces changes in adult animals consistent with those observed in MAM-treated rats on E17.

While a variety of neuroanatomical changes have been associated with schizophrenia, one recurring, although not uniformly replicated (Christison *et al*., 1989; Benes *et al*., 1991; Arnold *et al*., 1995) theme has been structural abnormalities of the hippocampal formation, including reduced regional volume and improper orientation of pyramidal cells compared with age-matched control subjects (Kovelman & Scheibel, 1984; Jonsson *et al*., 1997, 1999; Koolschijn *et al*., 2010). First degree relatives of individuals with schizophrenia have also been shown to exhibit some of the same cytoarchitectural abnormalities (Boos *et al*., 2007; Hao *et al*., 2009; Ho & Magnotta, 2010). The results of the present study confirm our earlier work showing that prenatal exposure to Ara-C results in a reproducible change in the cytoarchitectural features of the hippocampus including a thinning of CA1 and abnormal positioning of neurons in CA2/3 region (Elmer *et al*., 2004). There is a slight, but significant reduction in the number of CA1 pyramidal neurons that may be associated with a small decrease in the overall volume of the CA1 region. Although no volumetric changes were observed in the CA2/3 region of the hippocampus, there was a matching trend towards

decreased numbers of CA2/3 pyramidal neurons. These results, coupled with evidence for changes in the pattern of BrdU-labeled nuclear profiles throughout the hippocampus, indicates that gestational exposure to Ara-C decreases the number of cells in the hippocampus. Furthermore, there was a consistent finding of abnormal positioning of CA2/3 neurons in the surrounding molecular layer. The absence of BrdU-labeled nuclear profiles in this region suggests that the neuronal heterotopias in the CA2/3 region are not a direct effect of Ara-C on neurogenesis. Neuronal heterotopias have also been observed in the offspring of dams treated prenatally with MAM including in the dorsal CA1 region (Singh, 1977; Collier & Ashwell, 1993; Chevassus-Au-Louis *et al*., 1998). Developmental studies in MAM-treated rats suggest that the ectopic neurons migrate away from their normal positions postnatally, long after the initial exposure to the antimitotic agent (Singh, 1977). Furthermore, ectopic neurons in the hippocampus are integrated into functional neural networks and may form aberrant connections with the neocortex (Chevassus-Au-Louis *et al*., 1998). Although these studies administered MAM at earlier gestational ages (E14–E17), they raise the interesting possibility that early disruptions in neurogenesis lead to secondary disruptions in neuronal architecture and circuit formation. At this stage of our studies, it is not known if the neuronal ectopias associated with Ara-C treatment are caused by the same underlying factors as those associated with MAM. However, the two sets of studies suggest that environmental factors that disrupt neurogenesis may have diverse consequences from reducing cell number to disrupting neuronal cytoarchitecture and circuit formation.

Structural changes in the hippocampus of Ara-C-treated rats were accompanied by significant changes in MWM performance. This task provides a test of the behavioral consequences associated with a disruption of embryonic neurogenesis with particular relevance to the hippocampus, a structure that provides spatial and temporal context to executive function and working memory (Morris *et al*., 1982; Kesner *et al*., 1991; Stubley-Weatherly *et al*., 1996). Pronounced deficits in spatial navigation have also been described in Sprague-Dawley rats exposed to MAM (25 mg/kg) on E17 (Leng *et al*., 2005) and in people with schizophrenia performing virtual allocentric spatial navigation tasks (Hanlon *et al*., 2006; Weniger & Irle, 2008). Spatial reference memory was also significantly impaired in Ara-C-treated rats, as evidenced by a comparatively slow improvement in locating the fixed position of a submerged platform across trials during the training phase of the assay. In agreement with previous findings in the MAM model, AraC-treated rats showed a significantly longer latency to reach the target platform across consecutive training sessions than controls. Notably, a comparable dose of MAM (22 mg/kg) administered on E17 to male Wistar rats failed to produce similar deficits, suggesting that strain differences may influence the phenotypic expression of a prenatal disruption in neurogenesis. The changes observed in MWM performance in Sprague-Dawley rats treated on or after E17 do not reflect a non-specific sensorimotor deficit, in either Ara-C- (present study) or MAM-treated rats (Hazane *et al*., 2009) as there were no differences in the latency to discover the platform on the first day of training and rats had no difficulty locating it when it was visible.

Performance during the probe trial further highlighted spatial deficits in the Ara-C-treated rats. As a group, Ara-C-treated rats spent significantly less time searching for the platform in the correct quadrant or in exploring the vicinity of the previously located platform. The deficit was dependent on the start location and was most evident when rats were started in the north and, to a lesser extent, east quadrants of the maze. These data suggest that late gestational Ara-C treatment alters the animal's ability to use spatial information in learning the position of the hidden platform. The Ara-C-induced deficits in MWM performance observed in the present study are consistent with those observed following lesions of the hippocampal–prefrontal circuit (Moser *et al*., 1993; Wang & Cai, 2008). Although similarities between the performance deficits observed in Ara-C- and MAM-treated rats resemble those described in human subjects with schizophrenia performing a virtual spatial

learning task, additional studies are needed to determine whether hippocampal heterotopias, which are not consistently observed in the illness, contribute to the schizophreniform phenotype in animals.

In addition to changes in dorsal hippocampal function, rats exposed to Ara-C on E19.5 and E20.5 exhibited functional changes in a pathway connecting the ventrocaudal aspects of CA1/subiculum to the deep layers of the PrL-IL cortex (Jay & Witter, 1991; Jay *et al*., 1992). The hippocampal–mPFC pathway provides spatial and temporal context to working memory and executive function and is the principal anatomical substrate through which the mPFC gains access to memory processes (Doyere *et al*., 1993; Floresco *et al*., 1997; Izaki *et al*., 2000). Pathophysiological changes in synaptic plasticity and functional connectivity in the hippocampal–prefrontal network have been implicated as a potential target of dysfunction in schizophrenia and depression (Jay *et al*., 2004; Krach *et al*., 2010; Sigurdsson *et al*., 2010). The results of the present study have shown that exposure to the antimitotic drug Ara-C between E19.5 and 20.5 results in an attenuation of LTP, a canonical cellular model of learning and memory processing. The origin of the deficiency in these animals could have resulted from the cytoarchitectural changes in the hippocampus (Chevassus-Au-Louis *et al*., 1998) or a change in the cortical neurochemical milieu. It is well established that DA plays a modulatory role in the expression of LTP in this circuit (Jay *et al*., 2004) and that increases in cortical DA levels impair (Maroun & Richter-Levin, 2003; Rocher *et al*., 2004; Ishikawa *et al*., 2005; Xu *et al*., 2009) hippocampal–mPFC LTP. Notably, in the present study, cortical DA levels were increased by 58% in adult offspring of Ara-C-treated rats. While additional studies are needed to establish a causal link between the observed changes in DA and hippocampal–mPFC LTP, elevated cortical DA levels are a consistent finding in MAM-treated rats (Matsutani *et al*., 1980; Jonsson & Hallman, 1982; Hallman & Jonsson, 1984) where aberrant DA signaling has been attributed to a change in hippocampal excitability (Lodge & Grace, 2007; 2008).

The cytoarchitectural and functional changes observed following Ara-C administration on E19–20 are generally consistent with deficits observed in MAM-treated rats and at least some etiopathologic features of schizophrenia. As additional effort and resources are devoted to characterizing deficits in neurodevelopmental models, it will be important to ascertain which of these perturbations transcend the specific drug used to provoke them and to determine the optimal developmental age at which disruptions in neurogenesis lead to changes with maximal face validity. The results of the present study support the utility of Ara-C as an alternative antimitotic agent and point to the need to explore gestational ages beyond E17 as potential constructs for study of the cognitive changes occurring in schizophrenia.

Acknowledgments

We gratefully acknowledge the assistance of Dr Adam C. Puche with photomicroscopy. This study was supported by PHS grant MH076854 (M.W.V.). This article was prepared while M.W.V. was employed at the University of Maryland School of Medicine. The opinions expressed in this article are the authors' own and do not reflect the view of the National Institutes of Health, the Department of Health and Human Services, or the United States government.

Abbreviations

Ara-C	cytosine arabinoside
DA	dopamine
DOPAC	3,4-didyhydroxypheylacetic acid

E	embryonic day
LTP	long-term potentiation
MAM	methylazoxymethanol
mPFC	medial prefrontal cortex
MWM	Morris water maze
PND	postnatal day
PrL-IL	prelimbic–infralimbic cortex

References

Arnold SE, Franz BR, Gur RC, Gur RE, Shapiro RM, Moberg PJ, Trojanowski JQ. Smaller neuron size in schizophrenia in hippocampal subfields that mediate cortical-hippocampal interactions. Am J Psychiatry. 1995; 152:738–748. [PubMed: 7726314]

Bayer SA, Altman J, Russo RJ, Zhang X. Timetables of neurogenesis in the human brain based on experimentally determined patterns in the rat. Neurotoxicology. 1993; 14:83–144. [PubMed: 8361683]

Benes FM, Sorensen I, Bird ED. Reduced neuronal size in posterior hippocampus of schizophrenic patients. Schizophr Bull. 1991; 17:597–608. [PubMed: 1805353]

Boksa P. Of rats and schizophrenia. J Psychiatry Neurosci. 2007; 32:8–10. [PubMed: 17245468]

Boos HB, Aleman A, Cahn W, Hulshoff Pol H, Kahn RS. Brain volumes in relatives of patients with schizophrenia: a meta-analysis. Arch Gen Psychiatry. 2007; 64:297–304. [PubMed: 17339518]

Chevassus-Au-Louis N, Congar P, Represa A, Ben-Ari Y, Gaiarsa JL. Neuronal migration disorders: heterotopic neocortical neurons in CA1 provide a bridge between the hippocampus and the neocortex. Proc Natl Acad Sci USA. 1998; 95:10263–10268. [PubMed: 9707635]

Christison GW, Casanova MF, Weinberger DR, Rawlings R, Kleinman JE. A quantitative investigation of hippocampal pyramidal cell size, shape, and variability of orientation in schizophrenia. Arch Gen Psychiatry. 1989; 46:1027–1032. [PubMed: 2818140]

Collier PA, Ashwell KW. Distribution of neuronal heterotopiae following prenatal exposure to methylazoxymethanol. Neurotoxicol Teratol. 1993; 15:439–444. [PubMed: 8302246]

Courtney MJ, Coffey ET. The mechanism of Ara-C-induced apoptosis of differentiating cerebellar granule neurons. Eur J Neurosci. 1999; 11:1073–1084. [PubMed: 10103100]

Doyere V, Burette F, Negro CR, Laroche S. Long-term potentiation of hippocampal afferents and efferents to prefrontal cortex: implications for associative learning. Neuropsychologia. 1993; 31:1031–1053. [PubMed: 8290021]

Elmer GI, Sydnor J, Guard H, Hercher E, Vogel MW. Altered prepulse inhibition in rats treated prenatally with the antimitotic Ara-C: an animal model for sensorimotor gating deficits in schizophrenia. Psychopharmacology (Berl). 2004; 174:177–189. [PubMed: 14985933]

Esclaire F, Kisby G, Spencer P, Milne J, Lesort M, Hugon J. The Guam cycad toxin methylazoxymethanol damages neuronal DNA and modulates tau mRNA expression and excitotoxicity. Exp Neurol. 1999; 155:11–21. [PubMed: 9918700]

Fatemi SH, Folsom TD. The neurodevelopmental hypothesis of schizophrenia, revisited. Schizophr Bull. 2009; 35:528–548. [PubMed: 19223657]

Floresco SB, Seamans JK, Phillips AG. Selective roles for hippocampal, prefrontal cortical, and ventral striatal circuits in radial-arm maze tasks with or without a delay. J Neurosci. 1997; 17:1880–1890. [PubMed: 9030646]

Gmeiner WH, Skradis A, Pon RT, Liu J. Cytarabine-induced destabilization of a model Okazaki fragment. Nucleic Acids Res. 1998; 26:2359–2365. [PubMed: 9580686]

Hallman H, Jonsson G. Monoamine neurotransmitter metabolism in microencephalic rat brain after prenatal methylazoxymethanol treatment. Brain Res Bull. 1984; 13:383–389. [PubMed: 6149797]

Hanlon FM, Weisend MP, Hamilton DA, Jones AP, Thoma RJ, Huang M, Martin K, Yeo RA, Miller GA, Canive JM. Impairment on the hippocampal-dependent virtual Morris water task in schizophrenia. Schizophr Res. 2006; 87:67–80. [PubMed: 16844347]

Hao Y, Yan Q, Liu H, Xu L, Xue Z, Song X, Kaneko Y, Jiang T, Liu Z, Shan B. Schizophrenia patients and their healthy siblings share disruption of white matter integrity in the left prefrontal cortex and the hippocampus but not the anterior cingulate cortex. Schizophr Res. 2009; 114:128–135. [PubMed: 19643580]

Hazane F, Krebs MO, Jay TM, Le Pen G. Behavioral perturbations after prenatal neurogenesis disturbance in female rat. Neurotox Res. 2009; 15:311–320. [PubMed: 19384565]

Ho BC, Magnotta V. Hippocampal volume deficits and shape deformities in young biological relatives of schizophrenia probands. Neuroimage. 2010; 49:3385–3393. [PubMed: 19941961]

Ishikawa A, Kadota T, Kadota K, Matsumura H, Nakamura S. Essential role of D1 but not D2 receptors in methamphetamine-induced impairment of long-term potentiation in hippocampal-prefrontal cortex pathway. Eur J Neurosci. 2005; 22:1713–1719. [PubMed: 16197511]

Izaki Y, Hori K, Nomura M. Disturbance of rat lever-press learning by hippocampo-prefrontal disconnection. Brain Res. 2000; 860:199–202. [PubMed: 10727644]

Jay TM, Burette F, Laroche S. NMDA receptor-dependent long-term potentiation in the hippocampal afferent fibre system to the prefrontal cortex in the rat. Eur J Neurosci. 1995; 7:247–250. [PubMed: 7757261]

Jay TM, Rocher C, Hotte M, Naudon L, Gurden H, Spedding M. Plasticity at hippocampal to prefrontal cortex synapses is impaired by loss of dopamine and stress: importance for psychiatric diseases. Neurotox Res. 2004; 6:233–244. [PubMed: 15325962]

Jay TM, Thierry AM, Wiklund L, Glowinski J. Excitatory amino acid pathway from the hippocampus to the prefrontal cortex. contribution of AMPA receptors in hippocampo-prefrontal cortex transmission. Eur J Neurosci. 1992; 4:1285–1295. [PubMed: 12106392]

Jay TM, Witter MP. Distribution of hippocampal CA1 and subicular efferents in the prefrontal cortex of the rat studied by means of anterograde transport of Phaseolus vulgaris-leucoagglutinin. J Comp Neurol. 1991; 313:574–586. [PubMed: 1783682]

Jones CA, Watson DJ, Fone K. Animal models of schizophrenia. Br J Pharmacol. 2011; 164:1162–1194. [PubMed: 21449915]

Jonsson G, Hallman H. Response of central monoamine neurons following an early neurotoxic lesion. Bibl Anat. 1982:76–92. [PubMed: 6291505]

Jonsson SA, Luts A, Guldberg-Kjaer N, Brun A. Hippocampal pyramidal cell disarray correlates negatively to cell number: implications for the pathogenesis of schizophrenia. Eur Arch Psychiatry Clin Neurosci. 1997; 247:120–127. [PubMed: 9224904]

Jonsson SA, Luts A, Guldberg-Kjaer N, Ohman R. Pyramidal neuron size in the hippocampus of schizophrenics correlates with total cell count and degree of cell disarray. Eur Arch Psychiatry Clin Neurosci. 1999; 249:169–173. [PubMed: 10449591]

Kesner RP, Farnsworth G, Kametani H. Role of parietal cortex and hippocampus in representing spatial information. Cereb Cortex. 1991; 1:367–373. [PubMed: 1822746]

Koolschijn PC, van Haren NE, Cahn W, Schnack HG, Janssen J, Klumpers F, Hulshoff Pol HE, Kahn RS. Hippocampal volume change in schizophrenia. J Clin Psychiatry. 2010; 71:737–744. [PubMed: 20492835]

Kovelman JA, Scheibel AB. A neurohistological correlate of schizophrenia. Biol Psychiatry. 1984; 19:1601–1621. [PubMed: 6518211]

Krach S, Jansen A, Krug A, Markov V, Thimm M, Sheldrick AJ, Eggermann T, Zerres K, Stocker T, Shah NJ, Kircher T. COMT genotype and its role on hippocampal-prefrontal regions in declarative memory. Neuroimage. 2010; 53:978–984. [PubMed: 20060911]

Krasnova IN, Justinova Z, Ladenheim B, Jayanthi S, McCoy MT, Barnes C, Warner JE, Goldberg SR, Cadet JL. Methamphetamine self-administration is associated with persistent biochemical alterations in striatal and cortical dopaminergic terminals in the rat. PloS One. 2010; 5:e8790. [PubMed: 20098750]

Laroche S, Jay TM, Thierry AM. Long-term potentiation in the prefrontal cortex following stimulation of the hippocampal CA1/subicular region. Neurosci Lett. 1990; 114:184–190. [PubMed: 2395531]

Leng A, Jongen-Relo AL, Pothuizen HH, Feldon J. Effects of prenatal methylazoxymethanol acetate (MAM) treatment in rats on water maze performance. Behav Brain Res. 2005; 161:291–298. [PubMed: 15922056]

Lodge DJ, Grace AA. Aberrant hippocampal activity underlies the dopamine dysregulation in an animal model of schizophrenia. J Neurosci. 2007; 27:11424–11430. [PubMed: 17942737]

Lodge DJ, Grace AA. Hippocampal dysfunction and disruption of dopamine system regulation in an animal model of schizophrenia. Neurotox Res. 2008; 14:97–104. [PubMed: 19073417]

Lodge DJ, Grace AA. Gestational methylazoxymethanol acetate administration: a developmental disruption model of schizophrenia. Behav Brain Res. 2009; 204:306–312. [PubMed: 19716984]

Low NC, Hardy J. What is a schizophrenic mouse? Neuron. 2007; 54:348–349. [PubMed: 17481386]

Maroun M, Richter-Levin G. Exposure to acute stress blocks the induction of long-term potentiation of the amygdala-prefrontal cortex pathway in vivo. J Neurosci. 2003; 23:4406–4409. [PubMed: 12805280]

Matsutani T, Nagayoshi M, Tamaru M, Tsukada Y. Elevated monoamine levels in the cerebral hemispheres of microencephalic rats treated prenatally with methylazoxymethanol or cytosine arabinoside. J Neurochem. 1980; 34:950–956. [PubMed: 7359141]

Meyer U, Feldon J. Epidemiology-driven neurodevelopmental animal models of schizophrenia. Prog Neurobiol. 2010; 90:285–326. [PubMed: 19857543]

Moore H. The role of rodent models in the discovery of new treatments for schizophrenia: updating our strategy. Schizophr Bull. 2010; 36:1066–1072. [PubMed: 20870929]

Moore H, Jentsch JD, Ghajarnia M, Geyer MA, Grace AA. A neurobehavioral systems analysis of adult rats exposed to methylazoxymethanol acetate on E17: implications for the neuropathology of schizophrenia. Biol Psychiatry. 2006; 60:253–264. [PubMed: 16581031]

Morris R. Developments of a water-maze procedure for studying spatial learning in the rat. J Neurosci Methods. 1984; 11:47–60. [PubMed: 6471907]

Morris RG, Garrud P, Rawlins JN, O'Keefe J. Place navigation impaired in rats with hippocampal lesions. Nature. 1982; 297:681–683. [PubMed: 7088155]

Moser E, Moser MB, Andersen P. Spatial learning impairment parallels the magnitude of dorsal hippocampal lesions, but is hardly present following ventral lesions. J Neurosci. 1993; 13:3916–3925. [PubMed: 8366351]

Paxinos, G.; Watson, C. The Rat Brain in Stereotaxic Coordinates. 6th edn.. Academic Press; San Diego: 2007.

Rocher C, Spedding M, Munoz C, Jay TM. Acute stress-induced changes in hippocampal/prefrontal circuits in rats: effects of antidepressants. Cereb Cortex. 2004; 14:224–229. [PubMed: 14704220]

Sarraf CE, Ansari TW, Conway P, Notay M, Hill S, Alison MR. Bromodeoxyuridine-labelled apoptosis after treatment with antimetabolites in two murine tumours and in small intestinal crypts. Br J Cancer. 1993; 68:678–680. [PubMed: 8398692]

Sigurdsson T, Stark KL, Karayiorgou M, Gogos JA, Gordon JA. Impaired hippocampal-prefrontal synchrony in a genetic mouse model of schizophrenia. Nature. 2010; 464:763–767. [PubMed: 20360742]

Singh SC. Ectopic neurones in the hippocampus of the postnatal rat exposed to methylazoxymethanol during foetal development. Acta Neuropathol. 1977; 40:111–116. [PubMed: 930560]

Stubley-Weatherly L, Harding JW, Wright JW. Effects of discrete kainic acid-induced hippocampal lesions on spatial and contextual learning and memory in rats. Brain Res. 1996; 716:29–38. [PubMed: 8738217]

Talamini LM, Koch T, Luiten PG, Koolhaas JM, Korf J. Interruptions of early cortical development affect limbic association areas and social behaviour in rats; possible relevance for neurodevelopmental disorders. Brain Res. 1999; 847:105–120. [PubMed: 10564742]

Talamini LM, Koch T, Ter Horst GJ, Korf J. Methylazoxymethanol acetate-induced abnormalities in the entorhinal cortex of the rat; parallels with morphological findings in schizophrenia. Brain Res. 1998; 789:293–306. [PubMed: 9573386]

Vogel MW, Sinclair M, Qiu D, Fan H. Purkinje cell fate in staggerer mutants: agenesis versus cell death. J Neurobiol. 2000; 42:323–337. [PubMed: 10645972]

Wang GW, Cai JX. Reversible disconnection of the hippocampalprelimbic cortical circuit impairs spatial learning but not passive avoidance learning in rats. Neurobiol Learn Mem. 2008; 90:365–373. [PubMed: 18614383]

Weniger G, Irle E. Allocentric memory impaired and egocentric memory intact as assessed by virtual reality in recent-onset schizophrenia. Schizophr Res. 2008; 101:201–209. [PubMed: 18276116]

West MJ, Slomianka L, Gundersen HJ. Unbiased stereological estimation of the total number of neurons in thesubdivisions of the rat hippocampus using the optical fractionator. Anat Rec. 1991; 231:482–497. [PubMed: 1793176]

Xu TX, Sotnikova TD, Liang C, Zhang J, Jung JU, Spealman RD, Gainetdinov RR, Yao WD. Hyperdopaminergic tone erodes prefrontal long-term potential via a D2 receptor-operated protein phosphatase gate. J Neurosci. 2009; 29:14086–14099. [PubMed: 19906957]

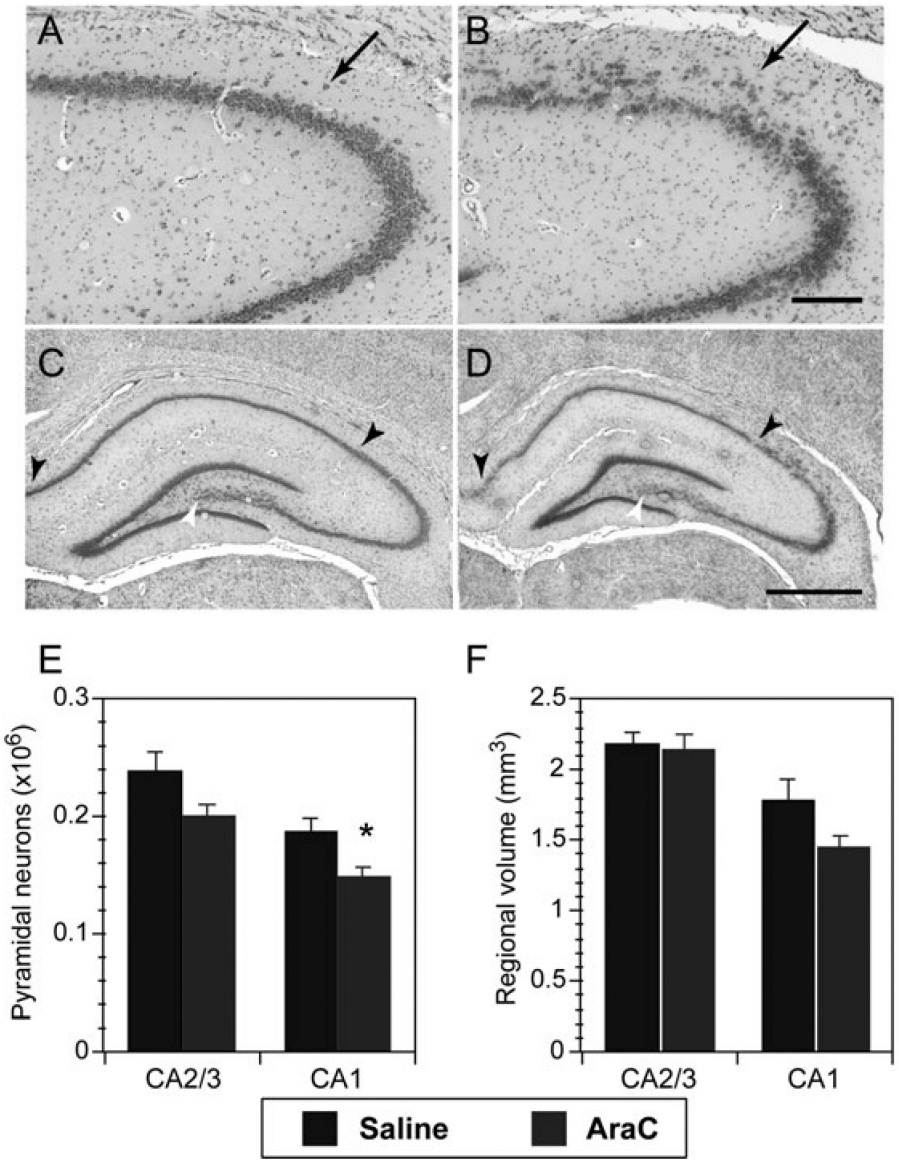

Fig. 1.

Cytoarchitectural changes in the hippocampus of Ara-C-treated rats. (A,B) Cresyl violet images of the CA2/3 regions of the dorsal hippocampus from control (A) and Ara-C-treated (B) rats to illustrate the disruption in the laminar organization of CA2/3 pyramidal neurons in Ara-C-treated rats (indicated by an arrowhead in B). Scale bar: 200 μm. (C–F) Pyramidal neuron cell counts and regional volume measurements in the hippocampus of adult rats treated with saline or Ara-C at E19.5 and 20.5. Cresyl violet images of the dorsal hippocampus from control (C) and Ara-C-treated (D) rats. Arrowheads and asterisks denote specific regions of CA1 and CA2/3, respectively, in the dorsal hippocampus used to compile cell counts. Scale bar: 1 mm. (E,F) Bar graphs illustrating the change in pyramidal cell number (C) and corresponding change in regional volume (D) of CA2/3 and CA1 region of the dorsal and ventral hippocampus. *$P < 0.05$, Student's *t*-test.

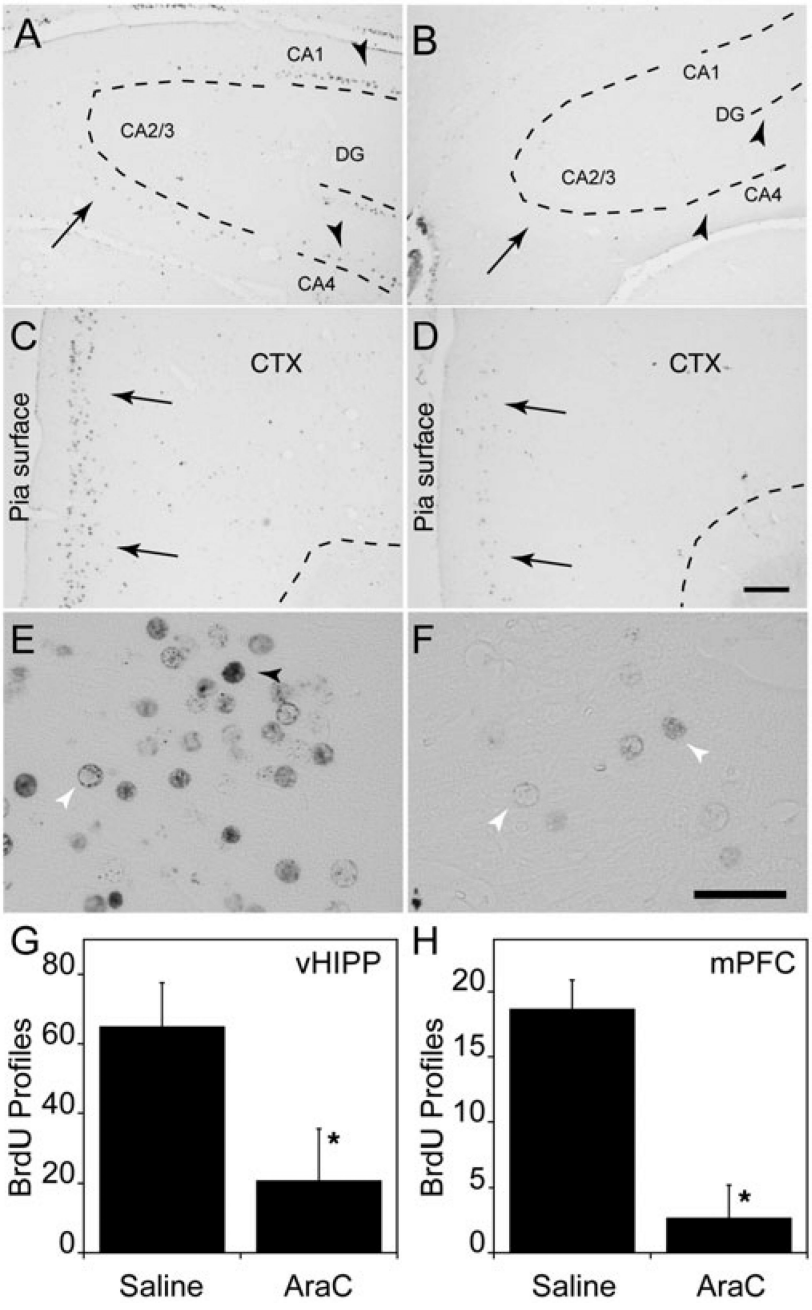

Fig. 2.

BrdU immunolabeling of the dorsal hippocampus and frontal cortex. (A,B) Representative coronal sections from the dorsal hippocampus. Arrowheads in A indicate BrdU-labeled nuclear profiles in the hilus and CA1 regions in saline-treated control rats (B). Note that the corresponding regions in Ara-C-treated rats are essentially devoid of BrdU-labeled profiles. The sparse BrdU labeling in the CA2/3 region of saline-treated rats (arrow) indicates that few neurons in this region were generated at the time of Ara-C injection (A). Note, however, that those few BrdU-labeled profiles in the CA2/3 region are missing in the Ara-C-treated rat. (C,D) BrdU labeling in the PrL-IL cortex. Although prominent BrdU immunolabeling of nuclear profiles was observed in saline-treated rats in the superficial cell layers of the cortex (C, arrows), only faint labeling of occasional nuclear profiles could be detected in Ara-C-

treated rats (D, arrows). The results suggest that many superficial layer neurons generated between E19.5 and E20.5 are missing in the Ara-C-treated rats. Scale bar: 500 μm (for A-D). (E,F) High magnification of BrdU immunoreactivity in the PrL-IL cortex of saline- (E) and Ara-C-treated rats (F). Both darkly labeled (black arrowhead) and lightly filled (white arrowhead) nuclear profiles are observed in saline-treated rats, while only lightly labeled BrdU profiles (white arrowheads) are observed in the Ara-C-treated rats. Scale bar: 10 μm. (G,H) Estimates of the number of BrdU-labeled profiles in the ventral hippocampus (G) and PrL-IL cortex (H) of saline- and AraC-treated rats. These regions correspond to the respective sites of electrical stimulation and recording in the LTP experiments. *$P < 0.05$.

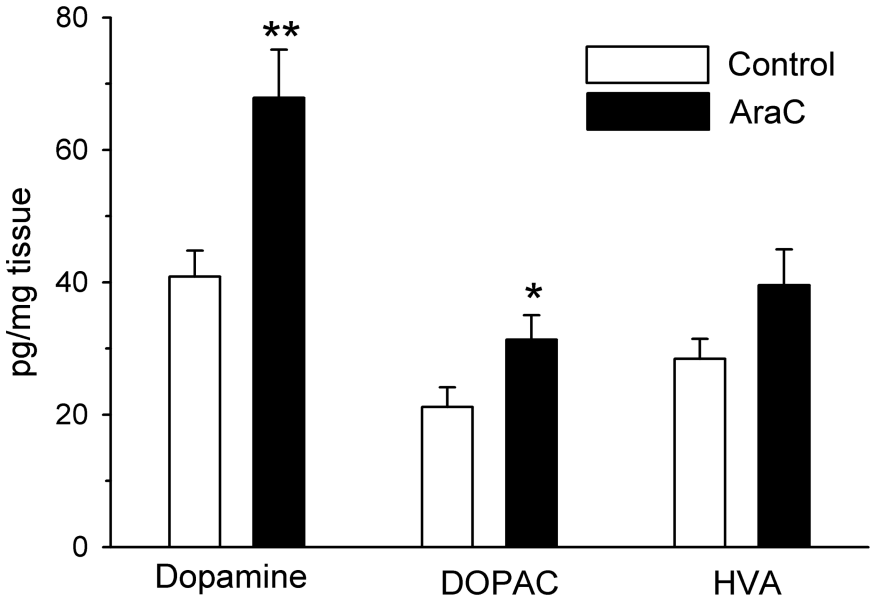

Fig. 3.

Effects of prenatal Ara-C exposure on DA, DOPAC and homovanillic acid levels in the cortex. Tissue levels, expressed in pg/mg of tissue were determined in extracts obtained from adult rats. $^{**}P < 0.005$, $^{*}P < 0.05$, Student's *t*-test.

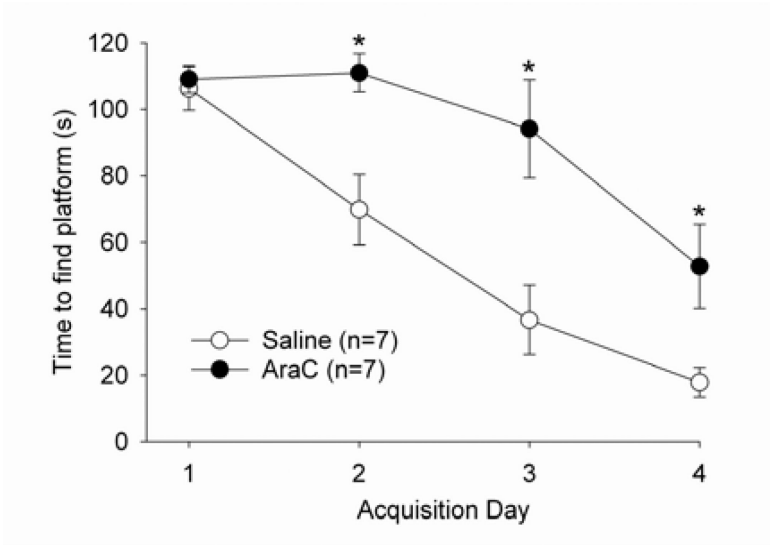

Fig. 4.

Acquisition phase of the Morris water maze task in saline- and Ara-C-treated rats. Both saline- (open circles) and Ara-C- (filled circles) treated rats improved performance across the 4-day acquisition of the task. However, saline-treated rats improved at a faster rate, with significantly faster times than Ara-C-treated rats on days 2, 3 and 4 (*P< 0.05, Fisher's LSD). No significant differences were observed between treatment groups on the first day of training.

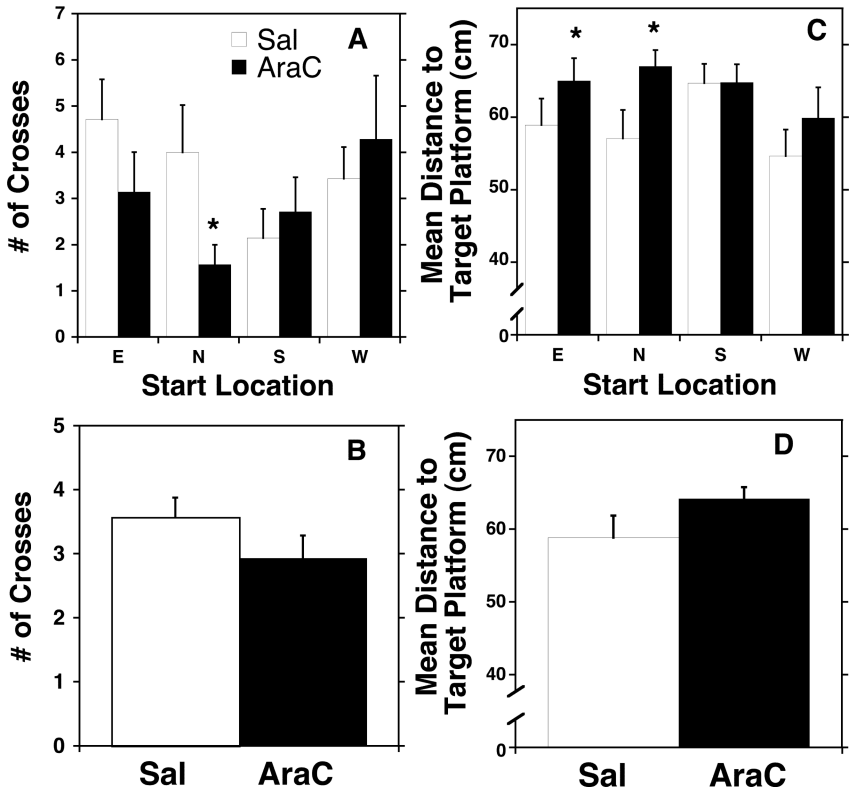

Fig. 5.

Effect of Ara-C treatment on exploration of the target platform's area in the probe trial of the Morris water maze test. Saline- (white) and Ara-C- (black) treated animals did not differ on performance in the probe test as measured by the number of crosses over the area formerly occupied by the platform (A) or the mean distance to the area formerly occupied by the target platform (C). However, when compared by start location, Ara-C rats did show significantly decreased platform crosses ($P<0.05$; B) and a greater mean distance to the target platform (N and E; * $P < 0.05$; D).

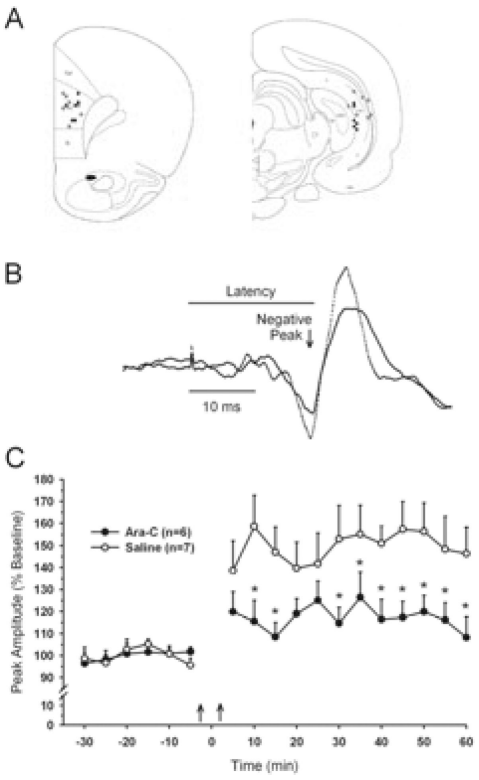

Fig. 6.

Ara-C-treated rats exhibit diminished expression of *in vivo* hippocampal–prefrontal cortex long-term potentiation. (A) Schematic representation of recording (left panel) and stimulating (right panel) electrodes from control (open circles) and Ara-C-treated (filled circles) rats. (B) Representative cortical field potentials evoked by test stimuli applied before (solid line) and after (dashed line) high-frequency stimulation of the CA1 region of the hippocampus. The peak amplitude (arrow) and latency to onset (horizontal line) of negative going component of the evoked potential was expressed as a percentage of an average value obtained prior to tetanic stimulation. (C) Comparison of the percentage change in the amplitude (mean ± SEM) of the negative component of the cortical evoked potential in saline- (open circles) and Ara-C-treated rats. Control rats showed a 50% increase in field potential amplitude following two tetanic train stimulations (onset indicated by two vertical arrows). By contrast, Ara-C-treated rats showed an approximately 20% increase in evoked potential amplitude. Group differences were significant at all but three time points (*$P <$ 0.05, Holm-Sidak).